

Versatile Physical Properties of a Novel Two-Dimensional Materials Composed of Group IV-V Elements

Seungjun Lee¹ and Young-Kyun Kwon^{1,*}

¹*Department of Physics and Research Institute for Basic Sciences,
Kyung Hee University, Seoul, 02447, Korea*

(Dated: March 1, 2022)

Abstract

Owing to the fascinating physical characteristics of two-dimensional (2D) materials and their heterostructure, much effort has been devoted to exploring their basic physical properties as well as discovering other novel 2D materials. Herein, based on first-principles calculations, we propose novel 2D material groups with the form A_2B_2 , composed of group IV ($A = \text{C, Si, Ge, or Sn}$) and V ($B = \text{N, P, As, Sb, or Bi}$) elements; the group forms two stable phases with the $P\bar{6}m2$ (\mathcal{M} phase) and $P\bar{3}m1$ (\mathcal{I} phase) crystal symmetries. We found that a total of 40 different freestanding A_2B_2 compounds were dynamically stable and displayed versatile physical properties, such as insulating, semiconducting, or metallic properties, depending on their elemental compositions. Our calculation results further revealed that the newly proposed 2D materials expressed high electrical and thermal transport properties. Additionally, some of the compounds that contained heavy elements exhibited non-trivial topological properties due to strong spin-orbit interactions.

I. INTRODUCTION

Graphene, the first two-dimensional (2D) material, exhibits fascinating physical properties, such as excellent transport properties,^{1,2} a very high mechanical strength,³ and a unique electronic structure with massless Dirac fermions.⁴ However, since the semi-metallic electronic structure of graphene severely limits its applications, enormous efforts have been devoted to discovering other 2D materials. As a result, a variety of 2D materials with sizable band gaps have been exfoliated from bulk materials. Examples of these new 2D materials include transition metal dichalcogenides (TMDCs),⁵⁻⁸ phosphorene,^{9,10} and hexagonal boron nitride (h-BN).¹¹⁻¹³ Furthermore, first-principles computational methods have also been successful in finding novel 2D materials and determining their physical properties.¹⁴⁻¹⁶

Intriguingly, the electron configurations in 2D semiconductors are distinguishable from bulk semiconductors. In three-dimensional (3d) semiconductors, atoms usually bond with the four nearest neighbors in an sp^3 tetrahedral structure; this satisfies the octet rule and disallows any dangling bonds or lone pairs of electrons. As a result, most 3D semiconductors either consist of single elements of group IV, such as Si or Ge, or consist of a combination of group III and V or II and VI elements with 1:1 stoichiometry. However, in 2D materials, lone pairs of electrons can be stabilized in the van der Waals gap between atomic layers. For example, the P in phosphorene and S in MoS_2 have three covalent bonds with the nearest neighbor and one lone pair of electrons pointing out of the atomic layer. Following the same rule, group III-VI and group IV-V compounds can also form 2D materials with sp^3 bonding structures, exhibiting interesting physical properties. Group III-VI 2D materials in the form of MX ($M = Ga$ or In ; $X = S, Se, \text{ or } Te$) have been reported to be semiconductors that exhibit interesting physical properties such as high electron mobility, anomalous optical responses, or topological phase transition by oxygen functionalization.^{17,18} As for the group IV-V compounds, several 2D crystal structures, such as that of the 2D carbon-phosphide group^{19,20}, SiP ²¹, GeP ^{22,23}, or $GeAs$ ²⁴, have been theoretically proposed and experimentally synthesized; however, comprehensive studies of 2D group IV-V compounds have not been conducted.

In this study, we used first-principles density functional theory to propose a novel 2D material group with the form of A_2B_2 , where A and B are elements in group IV (C, Si, Ge, or Sn) and group V (N, P, As, Sb, or Bi), respectively. This new material group contains

two distinct phases that possess inversion or mirror symmetry. We systematically studied the physical properties, such as geometrical structure, cohesive energy, phonon dispersion relation, and electronic structure of 40 kinds of 2D A_2B_2 materials. In addition, to explore the possible areas of application of the selected materials, we calculated their electrical and thermal transport properties and investigated their topological properties. Intriguingly, we found that 2D A_2B_2 semiconductors exhibit prominent electron and phonon transport properties, and some of the 2D A_2B_2 materials containing heavy elements exhibit topological non-trivial properties.

II. COMPUTATIONAL DETAILS

To investigate the electrical and vibrational properties of various A_2B_2 structure, we performed first-principles calculations based on density functional theory²⁵ and density functional perturbation theory (DFPT)²⁶ as implemented in the Quantum Espresso (QE) package.^{27,28} We employed the norm-conserving pseudopotentials²⁹ to describe the valence electrons, and treated exchange-correlation functional within the generalized gradient approximation of Perdew-Burke-Ernzerhof (PBE).³⁰ The plane-wave kinetic energy cutoff was selected to be 80 Ry, and $c = 20$ Å was chosen for the lattice constant of the direction perpendicular to the plane to mimic 2D structure. The Brillouin zone (BZ) of each structure was sampled using a $11 \times 11 \times 1$ k -point and $6 \times 6 \times 1$ q -point grid for the primitive unit cells of A_2B_2 . To explore transport properties in A_2B_2 , we solved the semi-classical Boltzmann transport equation (BTE) for both electrons and phonons. The carrier lifetimes are also calculated by density functional perturbation theory. We calculated anharmonic three phonon (3rd-order) interaction and electron-phonon interaction as scattering sources for phonons and electrons, respectively. To account for 3rd-order phonon interaction, we constructed $4 \times 4 \times 1$ supercell and calculated 3rd order inter-atomic force constants using finite-displacement approach.^{31–33} For the electron-phonon interaction, we calculated maximum localized Wannier function³⁴ and the electron-phonon matrix elements were initially calculated by $10 \times 10 \times 1$ coarse k - and q -points mesh and were interpolated to $100 \times 100 \times 1$ fine mesh by using EPW package³⁵. Note that the layer thickness of Si_2P_2 and C_2P_2 , which should be determined to evaluate the conductivity tensor, were chosen for 8.28 and 7.39 Å corresponding to half of out-of-plane lattice constants of their bulk configurations. The topological surface states

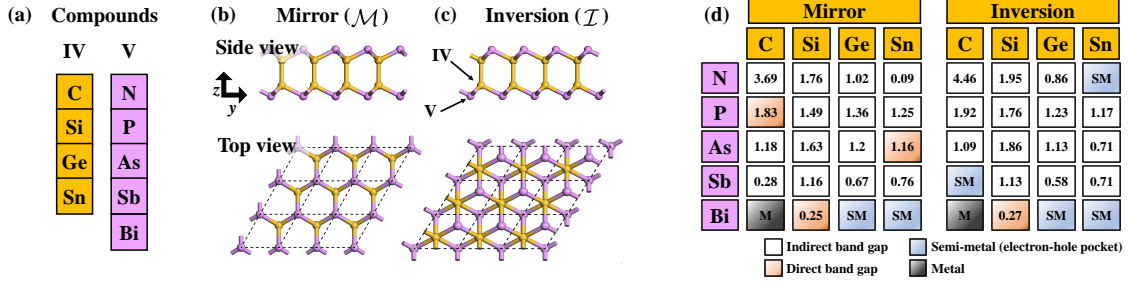


FIG. 1. (a) Group IV-V elements comprising the novel 2D materials. Side and top views of the equilibrium structures for two different phases: (b) mirror (\mathcal{M}) and (c) inversion (\mathcal{I}). The yellow and pink spheres represent the group IV and V elements, respectively, and the dashed line in the top view shows the primitive unit cell of the structure. (d) Electronic structure of A_2B_2 with the PBE functional. The white and orange boxes represent indirect and direct band gap semiconductors, respectively, with the band gaps measured in terms of electron volts. The sky blue and black boxes indicate semi-metallic and metallic electronic structures, respectively. For, A_2Bi_2 , we considered the spin-orbit coupling (SOC) effect due to strong the SOC strength in Bi; for the other cases, the SOC can be considered to be negligible.

and \mathbf{Z}_2 invariant were calculated by hybrid Wannier charge center method³⁶, and maximum localized Wannier function was obtained by WANNIER90 code.³⁴

III. RESULTS AND DISCUSSION

Based on first-principles calculations, we predicted 40 stable compounds formed by the group the IV element X (X=C, Si, Ge, or Sn) and group V element Y (Y=N, P, As, Sb, or Bi), with two different phases. Figure 1(a)-(c) show our newly proposed 2D structure (A_2B_2) and its compound elements. Depending on the position of the group V elements, A_2B_2 can form two different phases, one with the mirror symmetry (\mathcal{M} phase) and the other with inversion symmetry (\mathcal{I} phase). The crystal symmetries of the \mathcal{M} and the \mathcal{I} phases are $P\bar{6}m2$ and $P\bar{3}m1$, respectively, this relationship is similar to that between the $2H$ and $1T$ phases in TMDCs.^{5,6} We summarize the calculated equilibrium lattice constants in Table ???. The \mathcal{M} and \mathcal{I} phases have very similar lattice constants, and the constants are inversely proportional to the atomic numbers.

The dynamical stability of all the compounds was confirmed by calculating the phonon

dispersion relation. As shown in figures ?? (\mathcal{M} phase) and ?? (\mathcal{I} phase), there are no imaginary phonon frequencies except in the vicinity of the Γ point. For carbon-phosphide, it has been reported that the GaSe phase, similar to the \mathcal{M} phase, is the most stable configuration among the various compounds with 1:1 stoichiometry.³⁷ Therefore, we confirmed that 2D A_2B_2 is dynamically as well as energetically stable. To compare the structural stabilities of the \mathcal{M} and \mathcal{I} phases, we evaluated the cohesive energies of all the structures; they are summarized in Table ?. We found that in the systems that contain carbon atoms, the \mathcal{I} phase is more stable than the \mathcal{M} phase. In the systems that do not contain carbon atoms, the opposite is true.

To explore the physical properties of A_2B_2 , we investigated the electronic structures of all the compounds; the results are summarized in Figure 1(d). (Calculated band structures for all A_2B_2 compounds are presented in Figure ??.) We found that most A_2B_2 compounds are semiconductors, although some structures exhibit insulating or metallic properties. Interestingly, the heavier compounds exhibited smaller band gaps. Furthermore, if the atomic mass of A differed significantly from that of B, then A_2B_2 showed much smaller band gaps; some structures, such as $\mathcal{I}\text{-Sn}_2\text{N}_2$ or $\mathcal{I}\text{-C}_2\text{Sb}_2$, even became semi-metallic. We also note that for the heavier elements, SOC played an important role in determining the electronic structure. The SOC interaction can be considered negligible in A_2Sb_2 or Sn_2B_2 , but not in A_2Bi_2 . The effects of SOC on the A_2Bi_2 compounds will be discussed in a later section.

Carrier transport is one of the most important physical properties of semiconductors. In order to compare the transport properties of A_2B_2 with those of other 2D semiconductors, we calculated the electrical and thermal conductivities of Si_2P_2 and C_2P_2 ; these are composed of the elements most common in 2D semiconductors and have band gaps (1.49~1.92 eV) similar to those of other 2D semiconductors, such as phosphorene (0.88 eV)³⁸ and MoS_2 (1.9 eV).³⁹

The carrier mobilities of $\mathcal{M}\text{-Si}_2\text{P}_2$ and $\mathcal{M}\text{-C}_2\text{P}_2$ have been reported in previous theoretical work by W. Zhang et al⁴⁰. They used the Takagi formula⁴¹ to calculate the carrier mobilities, reporting huge values of room temperature carrier mobilities for $\mathcal{M}\text{-Si}_2\text{P}_2$ (46 ~ 8016 $\text{cm}^2\text{s}^{-1}\text{V}^{-1}$) and $\mathcal{M}\text{-C}_2\text{P}_2$ (498 ~ 39289 $\text{cm}^2\text{s}^{-1}\text{V}^{-1}$). However, the Takagi formula often significantly overestimates carrier mobilities in 2D materials.^{42?, 43} Therefore, to avoid overestimation, we calculated the electron-phonon interaction, which is a main scattering process in the semiconductor, for all band indices (i) and crystal momentums (\mathbf{k}), as shown

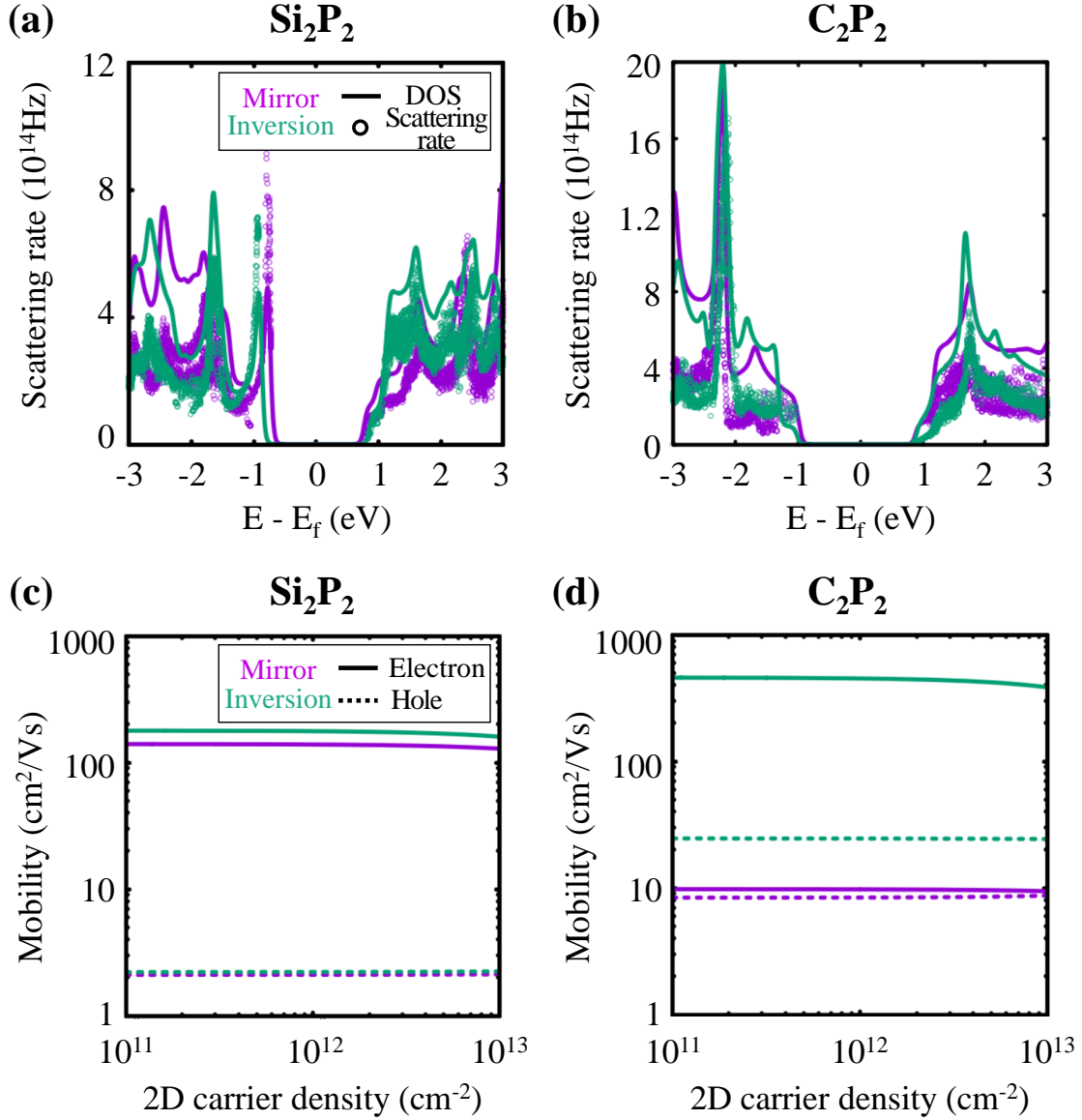


FIG. 2. Electron-phonon scattering rates of (a) Si_2P_2 and (b) C_2P_2 for \mathcal{M} (purple) and \mathcal{I} (cyan) phases with electron densities of states (solid lines). (c) and (d) show the calculated electron (solid line) and hole (dashed line) mobilities as functions of the 2D carrier concentrations of Si_2P_2 and C_2P_2 , respectively.

in Fig. 2(a, b). We followed the approach of Liao et al.⁴², accounting for the anisotropy of the matrix elements and nonparabolic band structures. According to Fermi's golden rule, the electron-phonon scattering rate must be proportional to the available final states, in other words, to the density of states (DOS). Thus, in both the Si_2P_2 and C_2P_2 , electrons

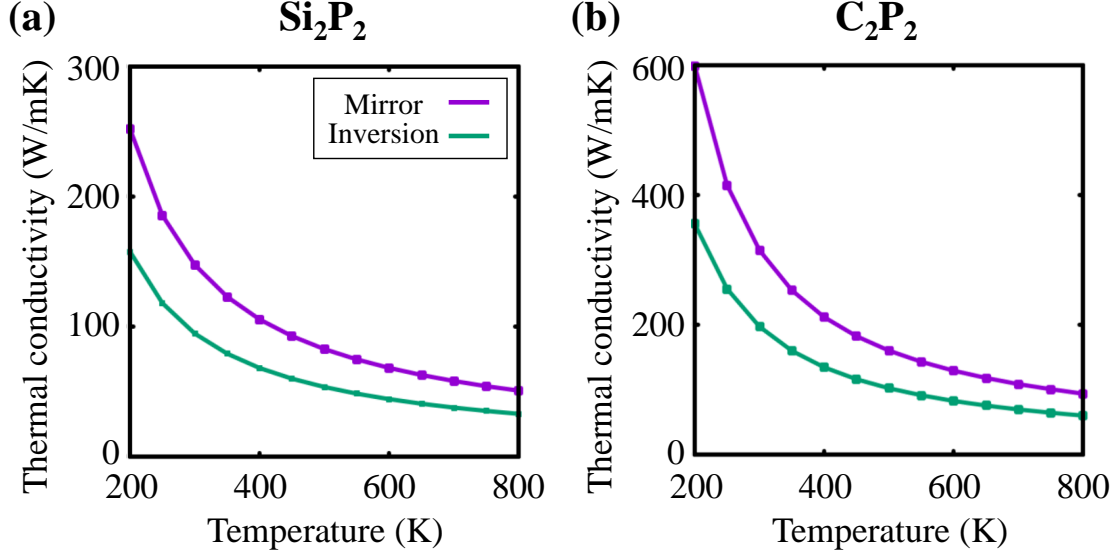


FIG. 3. Calculated lattice thermal conductivities of (a) Si₂P₂ and (b) C₂P₂ as functions of temperature ranging from 200 K to 800 K. The solid purple and cyan lines represent \mathcal{M} and \mathcal{I} phases, respectively.

have longer lifetimes than do holes, due to the lower DOS in the conduction bands. Based on the calculated carrier lifetimes, we investigated the room-temperature carrier mobilities of Si₂P₂ and C₂P₂ according to the carrier types and densities, as shown in Fig. 2(c, d). Due to the restriction of electron-phonon scattering in the conduction band, both Si₂P₂ and C₂P₂ showed higher carrier mobilities in the n doping region than in the p doping region. The calculated electron mobilities at a moderate carrier concentration (10^{12} cm^{-2}) are 139 and 177 $\text{cm}^2\text{s}^{-1}\text{V}^{-1}$ for \mathcal{M} - and \mathcal{I} -Si₂P₂, and 9.6 and 451 $\text{cm}^2\text{s}^{-1}\text{V}^{-1}$ for \mathcal{M} - and \mathcal{I} -C₂P₂, respectively. These values are comparable to or higher than those of other 2D materials calculated using the same method, such as phosphorene ($60\sim 170 \text{ cm}^2\text{s}^{-1}\text{V}^{-1}$)^{42?} and MoS₂ ($26 \text{ cm}^2\text{s}^{-1}\text{V}^{-1}$).⁴⁴ Therefore, newly proposed A₂B₂ compounds can be high performance n type 2D semiconductors, owing to their prominent transport properties.

The lattice thermal conductivity is also an important property in various applications such as thermoelectric devices. We calculated the lattice thermal conductivities of Si₂P₂ and C₂P₂ by solving the Boltzmann transport equation, as shown in Fig. 2(e, f). We found the room-temperature thermal conductivities to be 146 and 94 $\text{Wm}^{-1}\text{K}^{-1}$ for \mathcal{M} - and \mathcal{I} -Si₂P₂, and 313 and 196 $\text{Wm}^{-1}\text{K}^{-1}$ for \mathcal{M} - and \mathcal{I} -C₂P₂; these values are slightly larger than those of

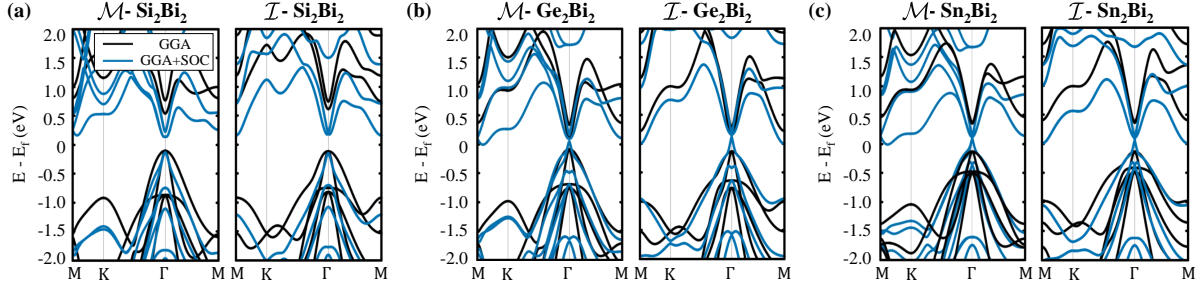


FIG. 4. Electronic structures of the \mathcal{M} and \mathcal{I} phases of (a) Si_2Bi_2 , (b) Ge_2Bi_2 , and (c) Sn_2Bi_2 , with (sky blue) and without (black) SOC.

other 2D materials, such as silicene ($26 \text{ Wm}^{-1}\text{K}^{-1}$),⁴⁵ MoS_2 ($23.2\sim 34.5 \text{ Wm}^{-1}\text{K}^{-1}$),^{46–48} or phosphorene ($65\sim 146 \text{ Wm}^{-1}\text{K}^{-1}$).⁴⁹ The relatively high thermal conductivities of Si_2P_2 and C_2P_2 imply that they cannot be good candidates for thermoelectric materials. However, we noticed that the same bonding characteristics of A_2B_2 may lead to a simple relation between the lattice thermal conductivity and atomic mass; thus, A_2B_2 covers a wide range of lattice thermal conductivities. Therefore, due to its versatile physical properties that depend on the compound elements, we believe that A_2B_2 can be used for various low-dimensional applications.

It has been reported that strong SOC in the low-dimensional system can lead to a topological phase transition via band inversion between the conduction and the valence bands.^{50,51} To further investigate the effects of SOC in A_2B_2 , we calculated the electronic structures of $\text{A}_2\text{Bi}_2\text{s}$ ($\text{A} = \text{Si, Ge, and Sn}$), which have a strong SOC strength due to Bi. Figures 4(a)-(c) show the electronic structures of A_2Bi_2 with and without SOC effects. Without the SOC interaction, $\text{A}_2\text{Bi}_2\text{s}$ are direct band gap semiconductors with sizable band gap values of $0.3\sim 0.8 \text{ eV}$. When the SOC was activated, the calculated band gap was greatly reduced. For example, the band gap of Si_2Bi_2 decreased from 0.8 eV to 0.3 eV . The band gaps of Ge_2Bi_2 and Sn_2Bi_2 were almost closed at Γ point, and the compounds exhibited semi-metallic electronic structures. Furthermore, the dispersion relation looked almost like linear band dispersion, similar to that of the Dirac cone structure.

To examine such an interesting dispersion relation in more detail, we scrutinized the band dispersion of $\mathcal{I}\text{-Sn}_2\text{Bi}_2$ near the Fermi level, as shown in Fig. 5(a). At the Γ point, we found a tiny band gap value of 0.02 eV . To understand the interesting dispersion relation

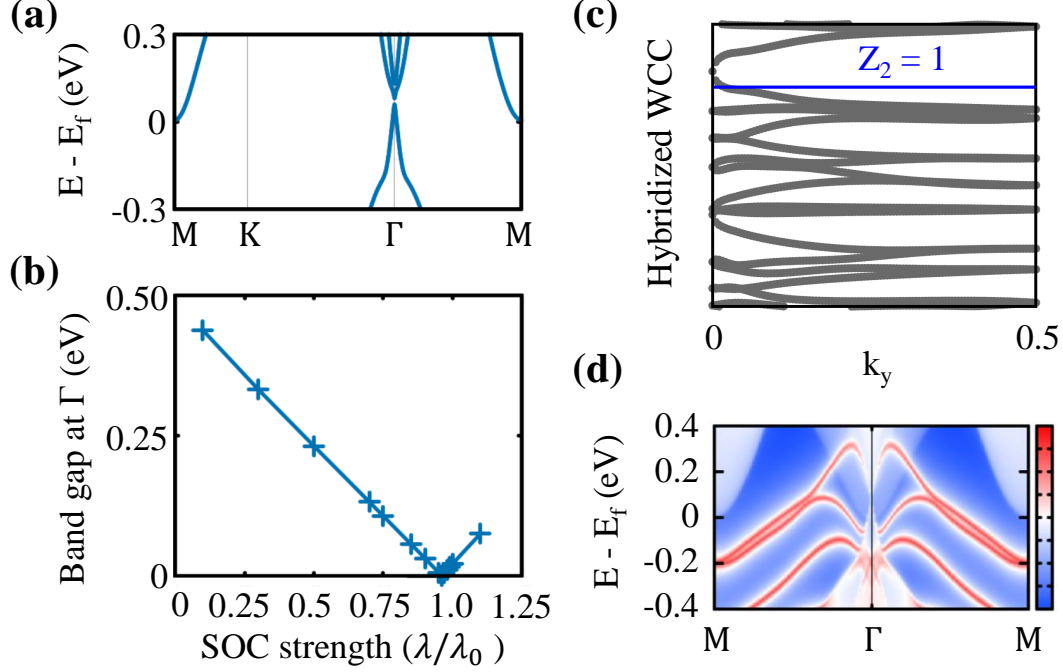


FIG. 5. (a) A close-up view of the band structure of \mathcal{T} -Sn₂Bi₂ near the Fermi level, including the SOC effect, (b) change in the band gap at Γ point, according to SOC strength λ , (c) evolution of hybridized Wannier charge center, and (d) surface band structure of \mathcal{T} -Sn₂Bi₂.

observed in \mathcal{T} -Sn₂Bi₂, we artificially manipulated the SOC strength (λ) and traced the band gap changes at the Γ point, as represented in Figure 5(b). We found that the band gap of \mathcal{T} -Sn₂Bi₂ decreases linearly with the increase of the λ and closes at $\lambda = 0.96\lambda_0$; after that point, the valence band and conduction band are reversed and the band gap linearly increases. It is well known that band inversion with a strong SOC interaction leads to a topological phase transition and the appearance of symmetry protected edge states.^{50,51} To confirm whether or not \mathcal{T} -Sn₂Bi₂ is a topological insulator, we calculated the \mathbf{Z}_2 invariant using the hybridized Wannier charge center (HWCC) method.³⁶ Figure 5 (c) shows the evolution of the HWCC with increasing \mathbf{k}_y . As plotted in Figure 5(c), an arbitrary horizontal line touches the HWCC an odd number of times, which means $\mathbf{Z}_2 = 1$. We also calculated the topological edge states of \mathcal{T} -Sn₂Bi₂ using the surface Green's function method for a semi-infinite system.⁵² Figure 5(d) shows the edge electronic structure of \mathcal{T} -Sn₂Bi₂, where a pair of edge states across the Fermi level moves from the valence band to the conduction band. Based on these results, we confirmed that \mathcal{T} -Sn₂Bi₂ is a 2D topological insulator. We also

revealed that \mathcal{M} - Sn_2Bi_2 is also a 2D topological insulator (See supplementary Figure ??). As for the other compounds, Ge_2Bi_2 and Si_2Bi_2 , they are topologically trivial because the SOC is not strong enough to close their relatively large band gaps. Nevertheless, since strain⁵³ or external fields⁵⁴ reduce the band gaps of 2D materials, Ge_2Bi_2 and Si_2Bi_2 may become 2D topological insulators under the correct perturbation .

IV. CONCLUSION

Based on first-principles density functional theory, we predicted a novel stable 2D material group, A_2B_2 , which is composed of group IV-V elements. The newly proposed IV-V compounds have two distinct stable phases—one with mirror symmetry (\mathcal{M} -phase), and the other with inversion symmetry (\mathcal{I} -phase). To explore the physical properties of these compounds, we evaluated the equilibrium structure, cohesive energy, phonon dispersion relations, electronic structure, and electrical and thermal transport properties including the phonon-mediated electron scattering rate and anharmonic phonon interaction. We found that depending on the combination of elements A and B, 2D A_2B_2 exhibits versatile physical properties such as large gap insulator, direct or indirect gap semiconductors, topological insulator, or metallic structure. Our results suggest that due to its fascinating physical properties, such as high-performance electronics and optoelectronics, the newly proposed 2D A_2B_2 can be used in various applications

* Corresponding author. E-mail: ykkwon@khu.ac.kr

¹ K. S. Novoselov, A. K. Geim, S. V. Morozov, D. Jiang, Y. Zhang, S. V. Dubonos, I. V. Grigorieva, and A. A. Firsov, *Science* **306**, 666 (2004).

² A. A. Balandin, S. Ghosh, W. Bao, I. Calizo, D. Teweldebrhan, F. Miao, and C. N. Lau, *Nano Lett.* **8**, 902 (2008).

³ C. Lee, X. Wei, J. W. Kysar, and J. Hone, *Science* **321**, 385 (2008), ISSN 0036-8075.

⁴ A. K. Geim and K. S. Novoselov, *Nat. Mater.* **6**, 183 (2007).

⁵ C. L. Tan and H. Zhang, *Chem. Soc. Rev.* **44**, 2713 (2015).

⁶ M. Chhowalla, H. S. Shin, G. Eda, L. J. Li, K. Loh, and H. Zhang, *Nat. Chem.* **5**, 263 (2013).

- ⁷ X. Huang, Z. Y. Zeng, and H. Zhang, Chem. Soc. Rev. **42**, 1934 (2013).
- ⁸ R. Lv, J. A. Robinson, R. E. Schaak, D. Sun, Y. Sun, T. E. Mallouk, and M. Terrones, Acc. Chem. Res. **48**, 56 (2015).
- ⁹ H. Liu, A. T. Neal, Z. Zhu, Z. Luo, X. Xu, D. Tománek, and P. D. Ye, ACS Nano **8**, 4033 (2014).
- ¹⁰ M. Akhtar, G. Anderson, R. Zhao, A. Alruqi, J. E. Mroczkowska, G. Sumanasekera, and J. B. Jasinski, npj 2D Mater. Appl. **1**, 5 (2017).
- ¹¹ Y. Lin, T. V. Williams, and J. W. S. Connell, J. Phys. Chem. Lett. **1**, 277 (2010).
- ¹² Q. Weng, X. Wang, X. Wang, Y. Bando, and D. Golberg, Chem. Soc. Rev. **45**, 3989 (2016).
- ¹³ L. H. Li and Y. Chen, Adv. Funct. Mater. **26**, 2594 (2016).
- ¹⁴ N. Mounet, M. Gibertini, P. Schwaller, D. Campi, A. Merkys, A. Marrazzo, T. Sohier, I. E. Castelli, A. Cepellotti, G. Pizzi, et al., Nat. Nanotechnol. **13**, 246 (2018), ISSN 1748-3395.
- ¹⁵ S. Haastrup, M. Strange, M. Pandey, T. Deilmann, P. S. Schmidt, N. F. Hinsche, M. N. Gjerding, D. Torelli, P. M. Larsen, A. C. Riis-Jensen, et al., 2D Mater. **5**, 042002 (2018).
- ¹⁶ K. Chae and Y.-W. Son, Nano Lett. **19**, 2694 (2019), ISSN 1530-6984.
- ¹⁷ D. A. Bandurin, A. V. Tyurnina, G. L. Yu, A. Mishchenko, V. Zólyomi, S. V. Morozov, R. K. Kumar, R. V. Gorbachev, Z. R. Kudrynskyi, S. Pezzini, et al., Nature Nanotechnol. **12**, 223 (2017), ISSN 1748-3395.
- ¹⁸ S. Zhou, C.-C. Liu, J. Zhao, and Y. Yao, npj Quantum Mater. **3**, 16 (2018), ISSN 2397-4648.
- ¹⁹ G. Wang, R. Pandey, and S. P. Karna, Nanoscale **8**, 8819 (2016), ISSN 20403372.
- ²⁰ J. Guan, D. Liu, Z. Zhu, and D. Tománek, Nano Letters **16**, 3247 (2016), ISSN 15306992.
- ²¹ C. Li, S. Wang, C. Li, T. Yu, N. Jia, J. Qiao, M. Zhu, D. Liu, and X. Tao, J. Mater. Chem. C **6**, 7219 (2018).
- ²² L. Li, W. Wang, P. Gong, X. Zhu, B. Deng, X. Shi, G. Gao, H. Li, and T. Zhai, Adv. Mater. **30**, 1706771 (2018).
- ²³ Z. Li, X. Shi, C. He, T. Ouyang, J. Li, C. Zhang, S. Zhang, C. Tang, R. A. Rmer, and J. Zhong, Appl. Surf. Sci. **497**, 143803 (2019), ISSN 0169-4332.
- ²⁴ C. S. Jung, D. Kim, S. Cha, Y. Myung, F. Shojaei, H. G. Abbas, J. A. Lee, E. H. Cha, J. Park, and H. S. Kang, J. Mater. Chem. A **6**, 9089 (2018).
- ²⁵ W. Kohn and L. J. Sham, Phys. Rev. **140**, A1133 (1965).
- ²⁶ S. Baroni, S. de Gironcoli, A. Dal Corso, and P. Giannozzi, Rev. Mod. Phys. **73**, 515 (2001).

- ²⁷ P. Giannozzi, S. Baroni, N. Bonini, M. Calandra, R. Car, C. Cavazzoni, D. Ceresoli, G. L. Chiarotti, M. Cococcioni, I. Dabo, et al., *J. Phys. Condens. Matter* **21**, 395502 (19pp) (2009).
- ²⁸ P. Giannozzi, O. Andreussi, T. Brumme, O. Bunau, M. B. Nardelli, M. Calandra, R. Car, C. Cavazzoni, D. Ceresoli, M. Cococcioni, et al., *J. Phys. Condens. Matter* **29**, 465901 (2017).
- ²⁹ D. R. Hamann, M. Schlüter, and C. Chiang, *Phys. Rev. Lett.* **43**, 1494 (1979).
- ³⁰ J. P. Perdew, K. Burke, and M. Ernzerhof, *Phys. Rev. Lett.* **77**, 3865 (1996).
- ³¹ A. Togo and I. Tanaka, *Scr. Mater.* **108**, 1 (2015).
- ³² W. Li, J. Carrete, N. A. Katcho, and N. Mingo, *Comp. Phys. Commun.* **185**, 1747 (2014).
- ³³ W. Li, L. Lindsay, D. A. Broido, D. A. Stewart, and N. Mingo, *Phys. Rev. B* **86**, 174307 (2012).
- ³⁴ A. A. Mostofi, J. R. Yates, G. Pizzi, Y.-S. Lee, I. Souza, D. Vanderbilt, and N. Marzari, *Comput. Phys. Commun.* **185**, 2309 (2014).
- ³⁵ S. Ponc, E. Margine, C. Verdi, and F. Giustino, *Comput. Phys. Commun.* **209**, 116 (2016), ISSN 0010-4655.
- ³⁶ Q. Wu, S. Zhang, H.-F. Song, M. Troyer, and A. A. Soluyanov, *Comput. Phys. Commun.* **224**, 405 (2018), ISSN 0010-4655.
- ³⁷ J.-C. Zheng, M. C. Payne, Y. P. Feng, and A. T.-L. Lim, *Phys. Rev. B* **67**, 153105 (2003).
- ³⁸ S.-H. Kang, J. Park, S. Woo, and Y.-K. Kwon, *Phys. Chem. Chem. Phys.* **21**, 24206 (2019).
- ³⁹ A. Kuc, N. Zibouche, and T. Heine, *Phys. Rev. B* **83**, 245213 (2011).
- ⁴⁰ W. Zhang, J. Yin, Y. Ding, Y. Jiang, and P. Zhang, *Nanoscale* **10**, 16750 (2018), ISSN 20403372.
- ⁴¹ S.-I. Takagi, A. Toriumi, M. Iwase, and H. Tango, *IEEE Trans. Electron. Dev.* **41**, 2357 (1994).
- ⁴² B. Liao, J. Zhou, B. Qiu, M. S. Dresselhaus, and G. Chen, *Phys. Rev. B* **91**, 235419 (2015).
- ⁴³ G. Gaddemane, W. G. Vandenberghe, M. L. Van de Put, S. Chen, S. Tiwari, E. Chen, and M. V. Fischetti, *Phys. Rev. B* **98**, 115416 (2018).
- ⁴⁴ F. Guo, Z. Liu, M. Zhu, and Y. Zheng, *Phys. Chem. Chem. Phys.* **21**, 22879 (2019).
- ⁴⁵ X. Gu and R. Yang, *J. Appl. Phys.* **117**, 025102 (2015).
- ⁴⁶ Y. Cai, J. Lan, G. Zhang, and Y.-W. Zhang, *Phys. Rev. B* **89**, 035438 (2014).
- ⁴⁷ B. Peng, H. Zhang, H. Shao, Y. Xu, X. Zhang, and H. Zhu, *RSC Adv.* **6**, 5767 (2016).
- ⁴⁸ R. Yan, J. R. Simpson, S. Bertolazzi, J. Brivio, M. Watson, X. Wu, A. Kis, T. Luo, A. R. Hight Walker, and H. G. Xing, *ACS Nano* **8**, 986 (2014).
- ⁴⁹ S. Lee, S.-H. Kang, and Y.-K. Kwon, *Sci. Rep.* **9**, 5149 (2019).
- ⁵⁰ X.-L. Qi and S.-C. Zhang, *Rev. Mod. Phys.* **83**, 1057 (2011).

- ⁵¹ M. Z. Hasan and C. L. Kane, Rev. Mod. Phys. **82**, 3045 (2010).
- ⁵² Q. Wu, S. Zhang, H.-F. Song, M. Troyer, and A. A. Soluyanov, Comput. Phys. Commun. **224**, 405 (2018), ISSN 0010-4655.
- ⁵³ E. Taghizadeh Sisakht, F. Fazileh, M. H. Zare, M. Zarenia, and F. M. Peeters, Phys. Rev. B **94**, 085417 (2016).
- ⁵⁴ Q. Liu, X. Zhang, L. B. Abdalla, A. Fazzio, and A. Zunger, Nano Lett. **15**, 1222 (2015).

Supplementary Information

Versatile Physical Properties of a Novel Two-Dimensional Materials Composed of Group IV-V Elements

Seungjun Lee¹ and Young-Kyun Kwon^{1,*}

¹*Department of Physics and Research Institute for Basic Sciences,
Kyung Hee University, Seoul, 02447, Korea*

(Dated: March 1, 2022)

TABLE S1. Lattice constant (\AA) of mirror and inversion phases of group IV-V compounds with primitive 2D hexagonal unit cells

	Mirror				Inversion			
	C	Si	Ge	Sn	C	Si	Ge	Sn
N	2.39	2.90	3.16	3.42	2.40	2.91	3.18	3.43
P	2.89	3.52	3.69	3.94	2.90	3.54	3.70	3.95
As	3.14	3.90	3.85	4.90	3.15	3.71	3.86	4.10
Sn	3.40	4.00	4.13	4.37	3.41	4.01	4.14	4.38
Bi	3.59	4.17	4.27	4.52	3.60	4.18	4.28	4.53

TABLE S2. Cohesive energies (eV/atom) of all compounds. Each value was calculated using the total energy differences between the group IV-V compounds and isolated atoms.

	Mirror				Inversion			
	C	Si	Ge	Sn	C	Si	Ge	Sn
N	-5.84	-5.44	-3.81	-3.61	-5.85	-5.43	-3.81	-3.60
P	-5.25	-4.19	-3.48	-3.27	-5.27	-4.19	-3.47	-3.26
As	-4.60	-3.81	-3.24	-3.07	-4.63	-3.80	-3.22	-3.06
Sn	-4.34	-3.54	-3.06	-2.90	-4.38	-3.52	-3.05	-2.89
Bi	-4.06	-3.31	-3.03	-2.79	-4.11	-3.31	-3.01	-2.77

* Corresponding author. E-mail: ykkwon@khu.ac.kr

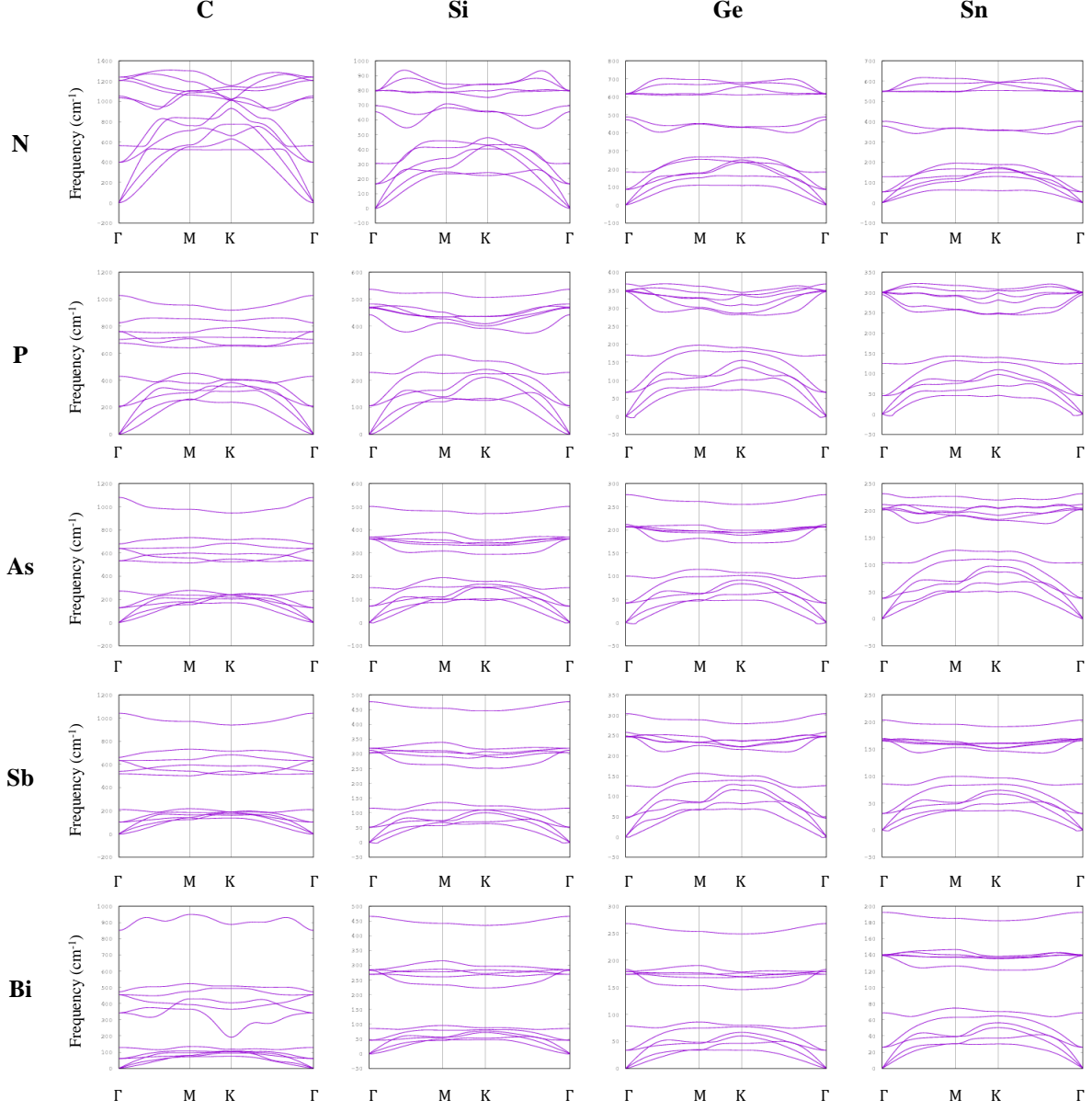


FIG. S1. Calculated phonon dispersion relations of \mathcal{M} -A₂B₂

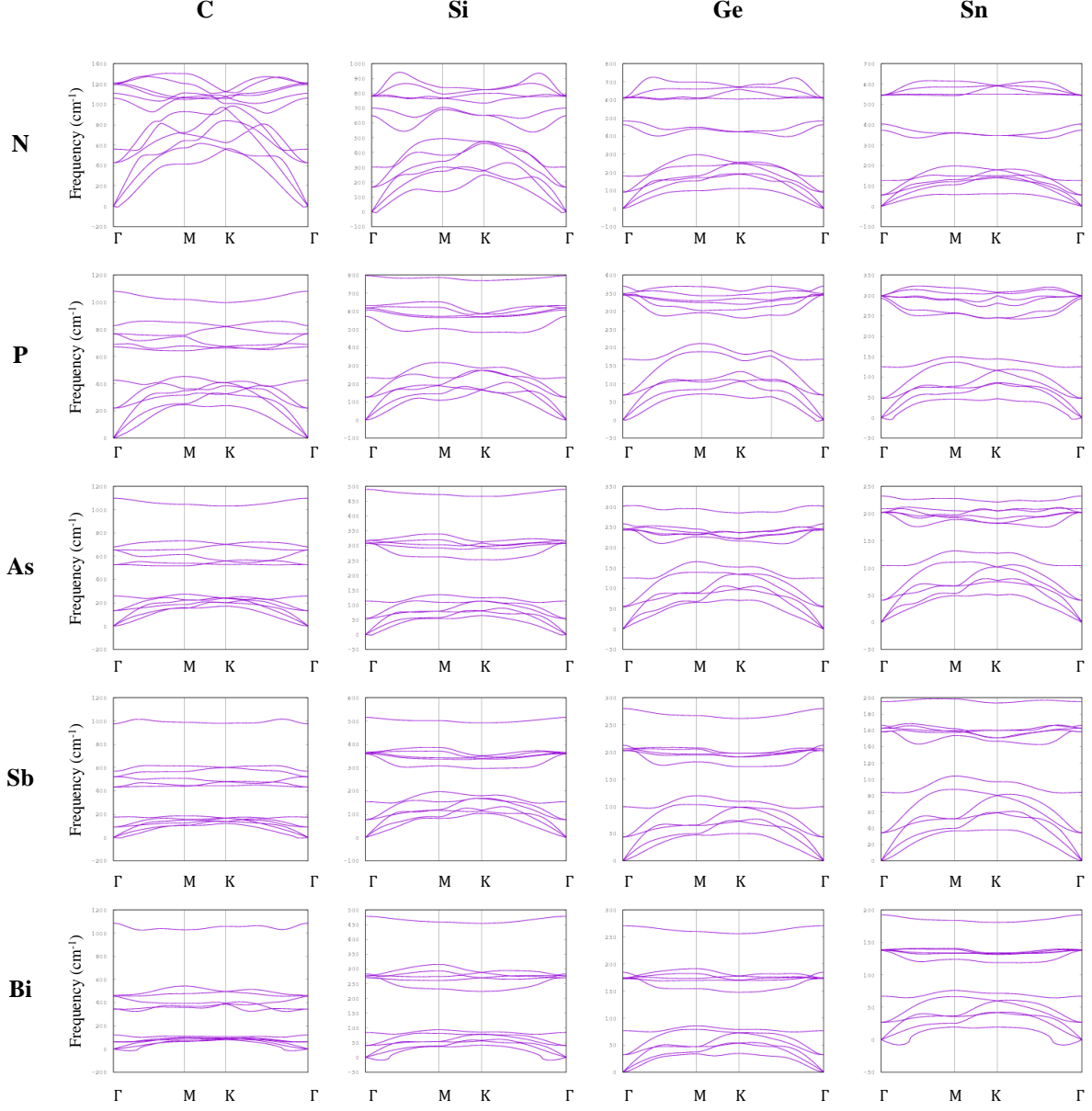


FIG. S2. Calculated phonon dispersion relations of \mathcal{I} -A₂B₂

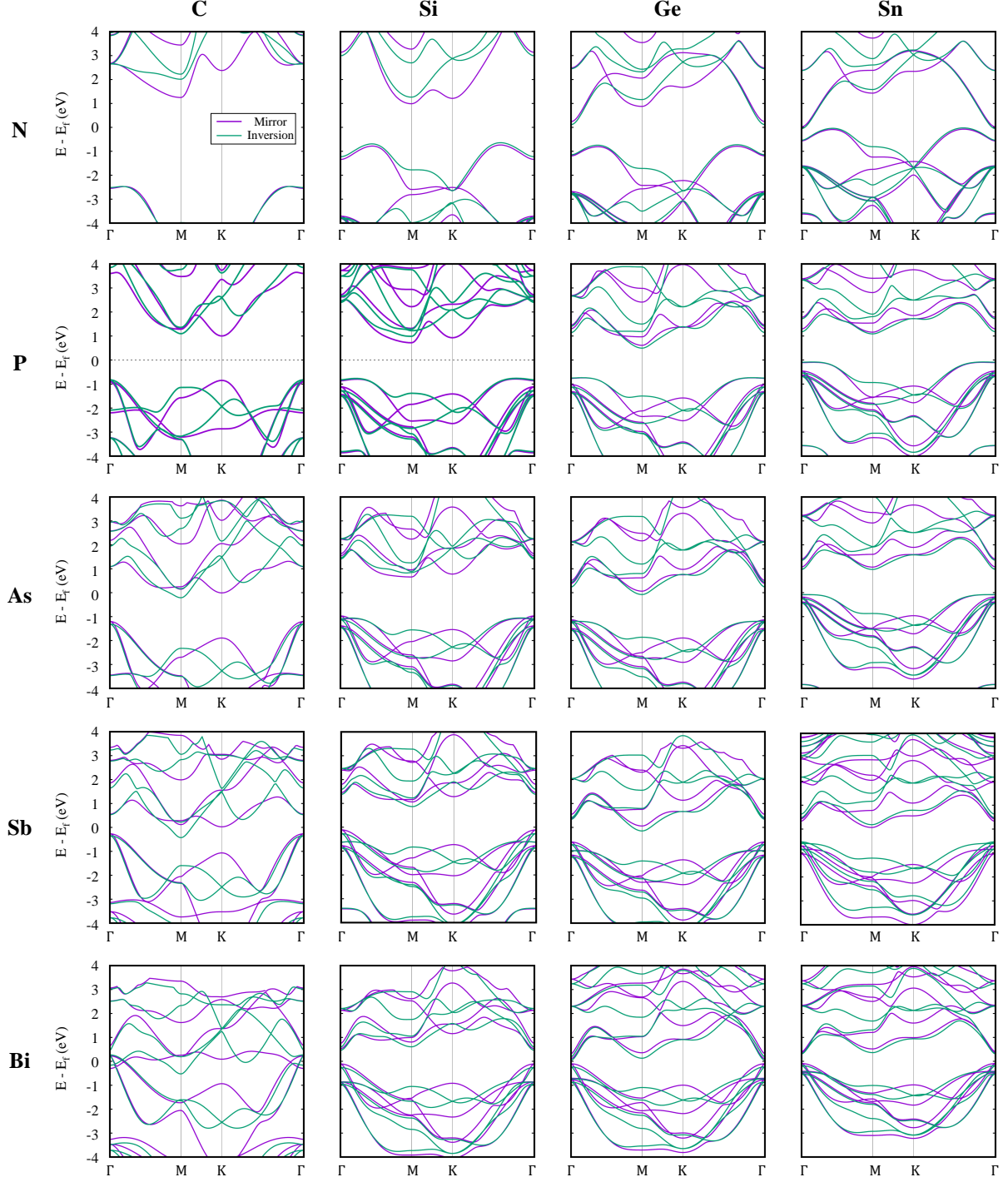


FIG. S3. Calculated band structures of \mathcal{M} - and \mathcal{I} - A_2B_2 . The purple and green lines indicate \mathcal{M} and \mathcal{I} phases, respectively.

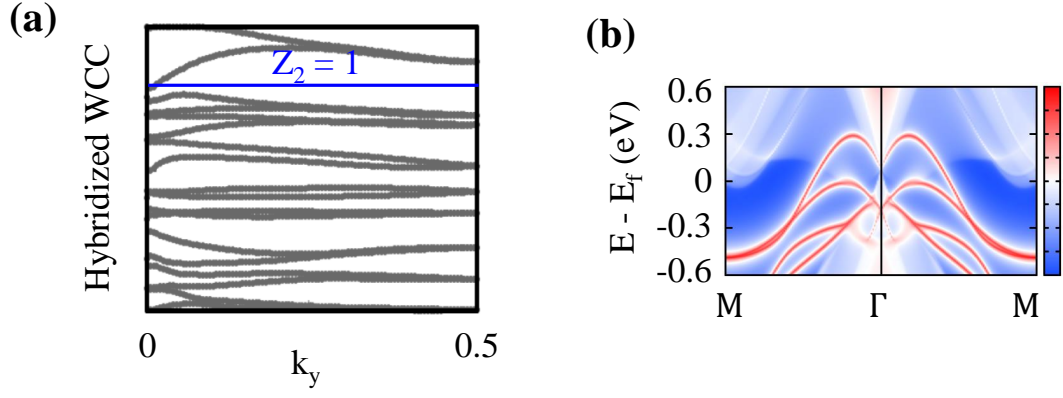


FIG. S4. (a) Evolution of the hybridized Wannier charge center, and (b) surface band structure of \mathcal{M} -Sn₂Bi₂.